

# Effects of Experimental Strabismus on the Architecture of Macaque Monkey Striate Cortex

SUZANNE B. FENSTEMAKER,<sup>1,2\*</sup> LYNNE KIORPES,<sup>2</sup> AND  
J. ANTHONY MOVSHON<sup>1,2</sup>

<sup>1</sup>Howard Hughes Medical Institute, New York University, New York, New York 10003

<sup>2</sup>Center for Neural Science, New York University,  
New York, New York 10003

---

---

## ABSTRACT

Strabismus, a misalignment of the eyes, results in a loss of binocular visual function in humans. The effects are similar in monkeys, where a loss of binocular convergence onto single cortical neurons is always found. Changes in the anatomical organization of primary visual cortex (V1) may be associated with these physiological deficits, yet few have been reported. We examined the distributions of several anatomical markers in V1 of two experimentally strabismic *Macaca nemestrina* monkeys. Staining patterns in tangential sections were related to the ocular dominance (OD) column structure as deduced from cytochrome oxidase (CO) staining. CO staining appears roughly normal in the superficial layers, but in layer 4C, one eye's columns were pale. Thin, dark stripes falling near OD column borders are evident in Nissl-stained sections in all layers and in immunoreactivity for calbindin, especially in layers 3 and 4B. The monoclonal antibody SMI32, which labels a neurofilament protein found in pyramidal cells, is reduced in one eye's columns and absent at OD column borders. The pale SMI32 columns are those that are dark with CO in layer 4. Gallyas staining for myelin reveals thin stripes through layers 2–5; the dark stripes fall at OD column centers. All these changes appear to be related to the loss of binocularity in cortical neurons, which has its most profound effects near OD column borders. *J. Comp. Neurol.* 438:300–317, 2001. © 2001 Wiley-Liss, Inc.

**Indexing terms:** visual cortex; cytochrome oxidase; ocular dominance

---

---

Strabismus, or a misalignment of the eyes, occurs naturally in human and monkey populations with a frequency of around 4% (Kiorpes and Boothe, 1980; von Noorden, 1980) and typically results in similar visual deficits in humans and monkeys (Kiorpes and Movshon, 1996). In some cases, strabismics become amblyopic, with degraded visual acuity in one eye. Invariably, there is a striking loss of binocular vision and a related directional asymmetry in the ability to track a moving object visually (Tychsen and Lisberger, 1986; Kiorpes et al., 1996). The binocular deficits in strabismics seem to result directly from a reduction in cortical binocular interaction, even though each eye is effective in driving cortical neurons (Hubel and Wiesel, 1965; Kiorpes et al., 1996).

Few anatomical studies report structural or functional changes in the visual cortex of animals with strabismus, yet some reorganization must underlie the changes in visual function. The loss of binocularity is evident in primary visual cortex (V1), suggesting that alterations caused by strabismus should be detected there. Prior to

the cortical level, and in layer 4C of V1, afferents from the two eyes are segregated. In normal monkeys, binocular combination of inputs onto single neurons first occurs in layers 4B and 3 (Lachica et al., 1992; Yoshioka et al., 1993) in the “interblob” regions surrounding the monocularly responsive cytochrome oxidase (CO) blobs. Tychsen and Burkhalter (1992) have reported that the horizontal connections between cells in adjacent ocular dominance columns in the superficial layers of V1 are altered in a naturally strabismic monkey. Specifically, connections between left and right eye columns are lost, leaving connections between same-eye columns intact. A similar pat-

---

Grant sponsor: National Eye Institute; Grant numbers: EY02017 and EY05864; Grant sponsor: Howard Hughes Medical Institute.

\*Correspondence to: Suzanne B. Fenstemaker, HHMI and New York University, Center for Neural Science, 4 Washington Place, Room 809, New York, NY 10003. E-mail: sue@cns.nyu.edu

Received 16 March 2001; Revised 20 June 2001; Accepted 20 June 2001

tern is evident in artificially strabismic cats, suggesting that the loss of horizontal connections is an effect rather than a cause of naturally occurring strabismus (Löwel and Singer, 1992). Neither the axonal nor the dendritic morphology of cortico-cortical projection neurons that remain in a naturally strabismic animal is significantly altered (Tychsen et al., 1996).

Given the disruption of binocular vision in strabismic monkeys, we have examined the distribution of several markers that are differentially expressed by neurons in the superficial layers of V1. In visually normal monkeys, these markers are preferentially associated with monocular or binocular eye dominance domains, or with functionally distinct classes of neurons.

**Cytochrome oxidase and NADPH diaphorase.** Tissue sections of V1 reacted to visualize the metabolic enzyme cytochrome oxidase (CO) show a distinctive pattern of dark patches or blobs in the superficial layers. These blobs overlie the centers of ocular dominance (OD) columns in the geniculate-recipient layer 4 and function as a marker for the most monocularly biased regions of the superficial layers (Horton, 1984). Histochemical reaction for a related enzyme, NADPH diaphorase, produces an exactly coincident pattern of neuropil staining (Sandell, 1986). Although CO does not appear to be associated with any particular classes of neurons, NADPH-diaphorase is found in the cell bodies and processes of  $\gamma$ -aminobutyric acid (GABA)ergic interneurons, and a class of large NADPH-containing interneurons is preferentially situated within CO blobs (Sandell, 1986). NADPH diaphorase is the same molecule as nitric oxide synthase (Dawson et al., 1991; Hope et al., 1991), and its expression has been shown to be activity-dependent in V1 (Sandell, 1986; Aoki et al., 1993). Expansion in strabismic monkeys of the blobs of neuropil staining or a change in number or distribution of NADPH-positive cell bodies may indicate altered local inhibitory interactions in binocular function.

**Calbindin.** A great variety of interneurons has been described in monkey V1, with virtually all sparsely spiny or aspiny neurons found to be GABAergic and presumably inhibitory. Dual labeling of these neurons indicates that in addition to nitric oxide synthase (NOS)/NADPH diaphorase, many of these GABAergic cells also contain one or more peptides, alone or in combination with one of the calcium binding proteins (Hendry et al., 1984; Jones et al., 1987; van Brederode et al., 1990). The vitamin D-dependent 28-kDa calcium binding protein calbindin is typically expressed by interneurons and is preferentially expressed in the interblob regions of V1, with a laminar pattern that is complementary to that of CO (van Brederode et al., 1990; Hendry and Carder, 1993; Carder et al., 1996). This distribution suggests that calbindin is associated with binocularly responsive neurons and a possible complement to NADPH diaphorase labeling. The expression of calbindin has been reported to be changed by visual form deprivation (Leclerc and Carder, 1994) as well as following monocular deprivation by impulse blockade (Carder et al., 1996).

**Neurofilament protein.** Pyramidal cells are the output neurons for neocortex; a reduction in the correlated binocular activation of these neurons might be reflected in reduced expression of structural proteins. Hendry and Bhandari (1992) have reported that structural protein expression is modifiable by activity. Specifically, monocular impulse blockade results in stripes of reduced MAP-2 immunoreactivity in layer 4C of V1 and in paler staining of rows of superficial

layer blobs. The pale rows coincide with the pale staining CO stripes and blobs and therefore represent a loss of the protein in the treated eyes' columns. Monocular deprivation of early onset causes a similar reduction in immunolabeling of neurofilament proteins in the deprived eye columns (Yoshioka et al., 1996).

A subclass of pyramidal cells in the superficial layers of V1 can be identified on the basis of immunoreactivity with the monoclonal antibody SMI32, which recognizes a nonphosphorylated epitope on the 168- and 200-kDa neurofilament subunits in somata and dendrites (Campbell and Morrison, 1989). These neurons are scattered across both blob and interblob domains in the superficial layers, and SMI32-immunoreactive apical dendrites bundle together in small clusters. Thus, changes in SMI32 expression by pyramidal cells might indicate regions of altered output from V1 arising from reduced binocular activation. Furthermore, a high proportion of the SMI32-immunoreactive neurons in visual cortex projects to the cortical motion processing area MT (Hof et al., 1996); in particular, dense SMI32 immunoreactivity is seen in layer 4B, a major source of projections to area MT. These patterns suggest an association of SMI32-immunoreactive neurons with the magnocellular lateral geniculate nucleus (LGN)-derived pathway for motion processing, and possibly with motion processing deficits in strabismic monkeys (Kiorpes et al., 1996).

We examined changes in the cortical distribution of these markers in two experimentally strabismic monkeys. The expression of calbindin, which is normally associated with regions of binocular activity, and Nissl staining are altered in these animals. Staining for NADPH diaphorase, which is normally associated with monocularly responsive regions of V1, is unchanged. A complicated pattern was found in immunoreactivity for SMI32, with reduced activity at OD column borders and more intense labeling within the central cores of the OD columns. Furthermore, we observed changes in CO activity, particularly in layer 4C. All these changes may be related to the lack of normal binocular activation in the strabismic visual cortex.

## MATERIALS AND METHODS

Strabismus was induced in two male *Macaca nemestrina* monkeys by surgical manipulation of the extraocular muscles at 9 days after birth. The left eyes of both animals were made esotropic, with the deviation in animal PW 20° and that in SY 25°. A complete report on the effects of artificial strabismus on pursuit eye movements and on neuronal responses in area MT in these animals has been published (Kiorpes et al., 1996). Both animals alternated fixation, and neither animal was amblyopic. Sections from two visually normal adult *M. nemestrina* were also processed to provide normal control material. These experiments were carried out under a protocol approved by the Animal Care and Use Committee of New York University and conformed to NIH guidelines for vertebrate use.

At the conclusion of the above-mentioned physiological recordings, the animals were given an intravenous overdose of sodium pentobarbital (65 mg/kg) and perfused with heparinized saline, followed by 4% paraformaldehyde in 0.1 M phosphate buffer. The brains were postfixed overnight in 4% paraformaldehyde at 4°C, and then the right occipital lobe was blocked coronally to allow examination of changes across the cortical layers. The left occipital operculum of each animal was removed as a single

sheet to be sectioned parallel to the cortical layers. This approach facilitates examination of changes across ocular dominance columns within a single layer. Following equilibration in 30% sucrose, frozen sections were cut at 40  $\mu\text{m}$  and processed according to standard methods for Nissl staining or for demonstrating cytochrome oxidase (Wong-Riley, 1979) or NADPH diaphorase (Sandell, 1986), for myelinated fibers (Gallyas, 1979), or for immunocytochemical labeling.

Immunocytochemical sections were incubated free-floating for 30 minutes in 1% bovine serum albumin (BSA) in Tris-buffered saline (TBS) containing 0.3% Triton-X100 to block non-specific labeling and to permeabilize the sections. They were rinsed in TBS and incubated in either a monoclonal antibody directed against calbindin-d (dilution of 1:2,000; Sigma, St. Louis, MO) or against a non-phosphorylated epitope on 168- and 220-kDa neurofilament proteins (SMI32, dilution of 1:10,000; Sternberger Monoclonals, Lutherville, MD) overnight at room temperature. The sections were rinsed in TBS, incubated for 2 hours in biotinylated secondary antibodies (Vector, Burlingame, CA) at dilutions of 1:200, and visualized by the ABC detection system (Vector) using diaminobenzidine (DAB) or 3-amino-9-ethylcarbazole (AEC) (Vector) as the chromogen.

Some unstained sections were mounted and temporarily coverslipped with glycerol for photography; these sections were subsequently stained for Nissl substance. The tissue was examined, some reconstructions were performed using an Olympus BHS microscope equipped with a camera lucida, and photomicrographs were made with a Zeiss Axiophot microscope. Photographic negatives were digitized, and low-power images of tissue sections were obtained by using the transparency module of an Agfa Duo-Scan flatbed scanner, controlled by a Power Macintosh running Adobe Photoshop. Photoshop was also used to enhance image contrast prior to analysis. The public domain NIH Image program (modified by James Cavanaugh of the Center for Neural Science, New York University) was used to align section images using radial blood vessels as reference points and to measure ocular dominance columns. Counts of Nissl-stained cells from adjacent series of dark and light stripes in layer 3 were made using a camera lucida. Every stained nucleus contained within a 100- $\mu\text{m}^2$  box centered on a dark or pale stripe was included; we made no attempt to distinguish neurons from glia. Nuclei that touched either of two sides of this box were included, whereas nuclei touching either of the remaining two sides were excluded. Final images were assembled using Adobe Photoshop and were printed at 300 dpi on a Kodak 8650 dye sublimation printer.

## RESULTS

Figure 1 illustrates the distribution of the major markers we examined in the superficial layers of V1 of a visually normal monkey. The sections were taken from a physically flattened operculum. The left-hand column shows calbindin immunoreactivity (top), CO staining (middle), and SMI32 immunoreactivity (bottom) from adjacent sections. In the middle column, regions of intense CB immunoreactivity, the centers of CO blobs, and patches of intense SMI32 immunoreactivity have been colored green, red, and yellow, respectively. The upper rightmost panel shows the superimposition of the CB and CO labeling, with regions of overlap indicated in blue. As reported

previously (Celio et al., 1986; van Brederode et al., 1990; Hendry and Carder, 1993), calbindin immunoreactivity tends to form a matrix around the CO blobs, with only minimal overlap. The lower rightmost panel shows the superimposition of SMI32 and CO, also with regions of overlap indicated by blue. The numerous blue patches suggest that the SMI32 immunoreactivity is distributed within the blobs as well as in the interblobs. There is no discernable correlation with the blob pattern.

## Cytochrome oxidase and NADPH diaphorase

When viewed in a flat-mounted section of V1, dense CO reactivity forms regular blobs that are sometimes connected by bridges within a row. These rows correspond to the centers of ocular dominance columns and they have a typical center-to-center spacing of about 0.4 mm (Horton, 1984). Layer 4A is marked by a "honeycomb" pattern, with no OD pattern visible. Staining is uniformly sparse in 4B and dense in 4C, with 4C $\beta$  often darker than 4C $\alpha$ . Faint blobs are visible in lightly stained layer 5 and in darkly stained layer 6. Figure 2 illustrates the CO staining obtained in tangential sections through opercular V1 of strabismic monkey PW. In the superficial layers, the sizes of blobs in adjacent rows are similar and appear relatively normal. Sections taken through the middle layers from PW shows that stripes are visible through layers 4A, 4B, and 4C; these stripes are illustrated in Figure 3. Similar, but somewhat less distinct stripe patterns are seen in monkey SY (Fig. 2C; arrows mark layer 4C $\beta$  stripes). No inhomogeneities are visible in layer 4 in coronal sections from monkey PW (Fig. 2D).

In monkey SY, (Fig. 2C) the CO blobs are smaller than those in PW. In some regions of superficial layer 3 the blobs even appear to be split into two, but these pairs occupy columns with the same center spacing. CO blob spacing in strabismic monkeys (including PW and SY), which we have reported separately, is not significantly different from that seen in visually normal monkeys (Murphy et al., 1998).

Figure 3 illustrates the relation of the layer 4 stripe patterns to the superficial layer blobs (Fig. 3A); the region shown is that marked by the white box in Figure 2A. In strabismic animals, the honeycomb pattern in layer 4A is interrupted by thin pale stripes (Fig. 3B). The dark portions of the honeycomb are aligned with each row of superficial-layer blobs (Fig. 3A-C) and have center to center spacing of about 0.4 mm and widths of about 0.3 mm. These are normal values for ocular dominance column spacing (Horton and Hocking, 1996b), and the densely stained regions may mark the most monocular central core of the columns (Horton, 1984). CO staining in layer 4C $\alpha$  is generally uniform and dark. The pattern in most of layer 4C $\beta$ , however, resembles that of a monocularly enucleated monkey (Fig. 3C,D), with dark and light stripes of approximately equal width; the dark stripes (marked by white arrows) are aligned with alternate rows of blobs and stripes in the more superficial layers. Thus, the OD columns of one eye are pale in 4C $\beta$ . This contrasts with the pattern in layer 4A in which each eye's core region is dark. Panels D and E of Figure 3 show the stripes of layer 4C in more detail; the region illustrated is that marked by the black box in Figure 2B and is just ventral to that in panels A-C. The dark stripes in the deepest portion of 4C $\beta$  appear to be split into two thin stripes (Fig. 3E, white asterisks), but they are still restricted to one eye's columns.

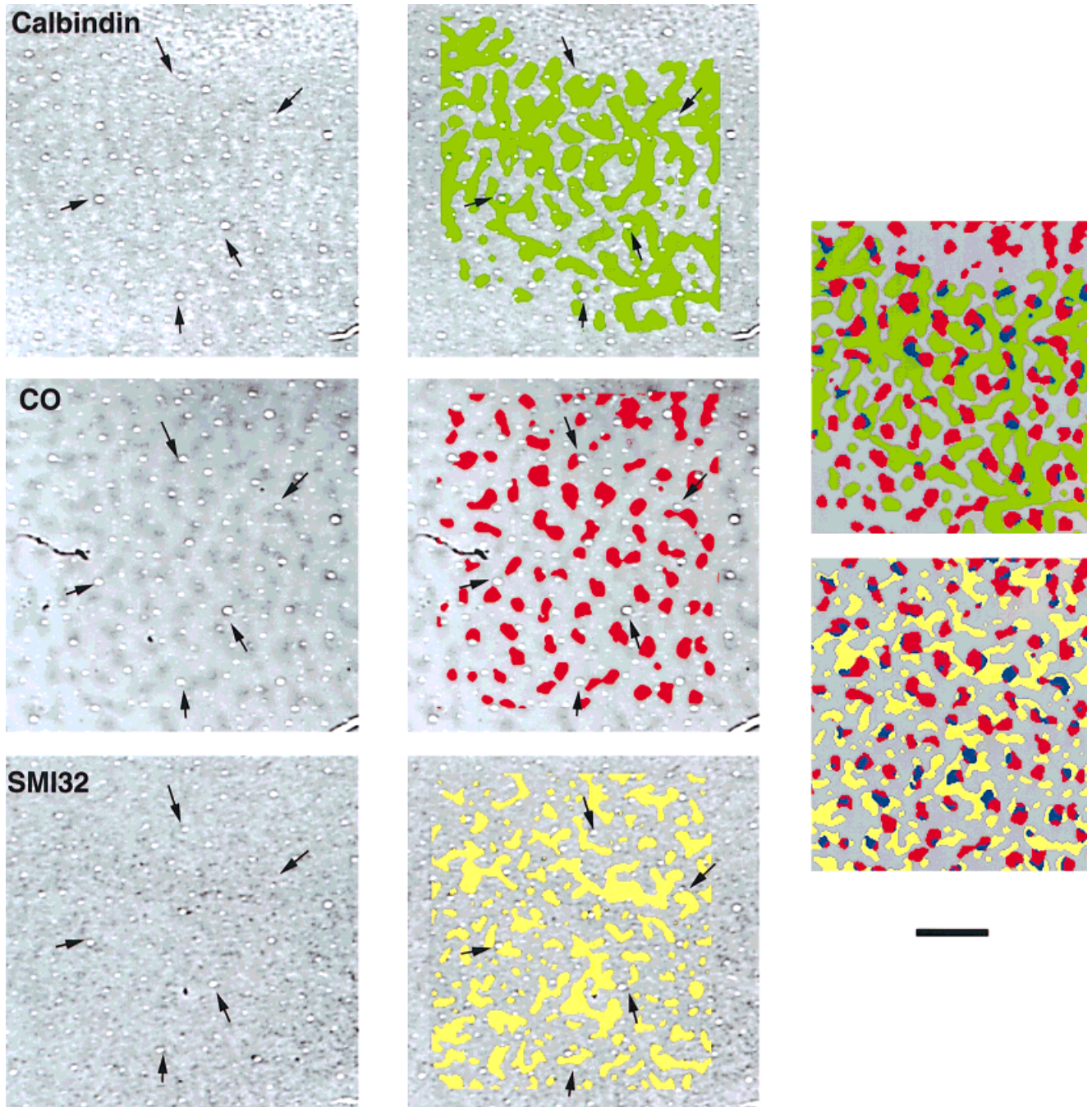


Fig. 1. The distribution in superficial layers of normal monkeys of calbindin immunoreactivity (top left), SMI32 neurofilament protein immunoreactivity (bottom left), and their relation to the CO blobs (center left), which mark the centers of OD columns. Serial sections are cut parallel to the cortical layers from a flattened block of oper-

cular V1. Arrows mark the same blood vessels in each section. Middle panel shows regions of intense CB (yellow), CO (red), and SMI32 (green). The rightmost panels are superimpositions of CB and CO (top), and SMI32 and CO (bottom). Blue areas indicate colocalization of CO and CB or SMI32. Scale bar = 1 mm.

Faint blobs with normal spacing are visible in layers 5 and 6; the apparent orientation of the string of blobs differs from that seen in the superficial layers.

Staining for NADPH diaphorase revealed a pattern of superficial layer blobs, as well as stripes in layer 4. The patterns were of slightly higher contrast than in the CO-

stained material, but the patterns in the NADPH diaphorase sections were indistinguishable from those obtained with CO.

#### Nissl staining

Normal Nissl staining is uniform within a single cortical layer. In flattened sections from strabismic mon-

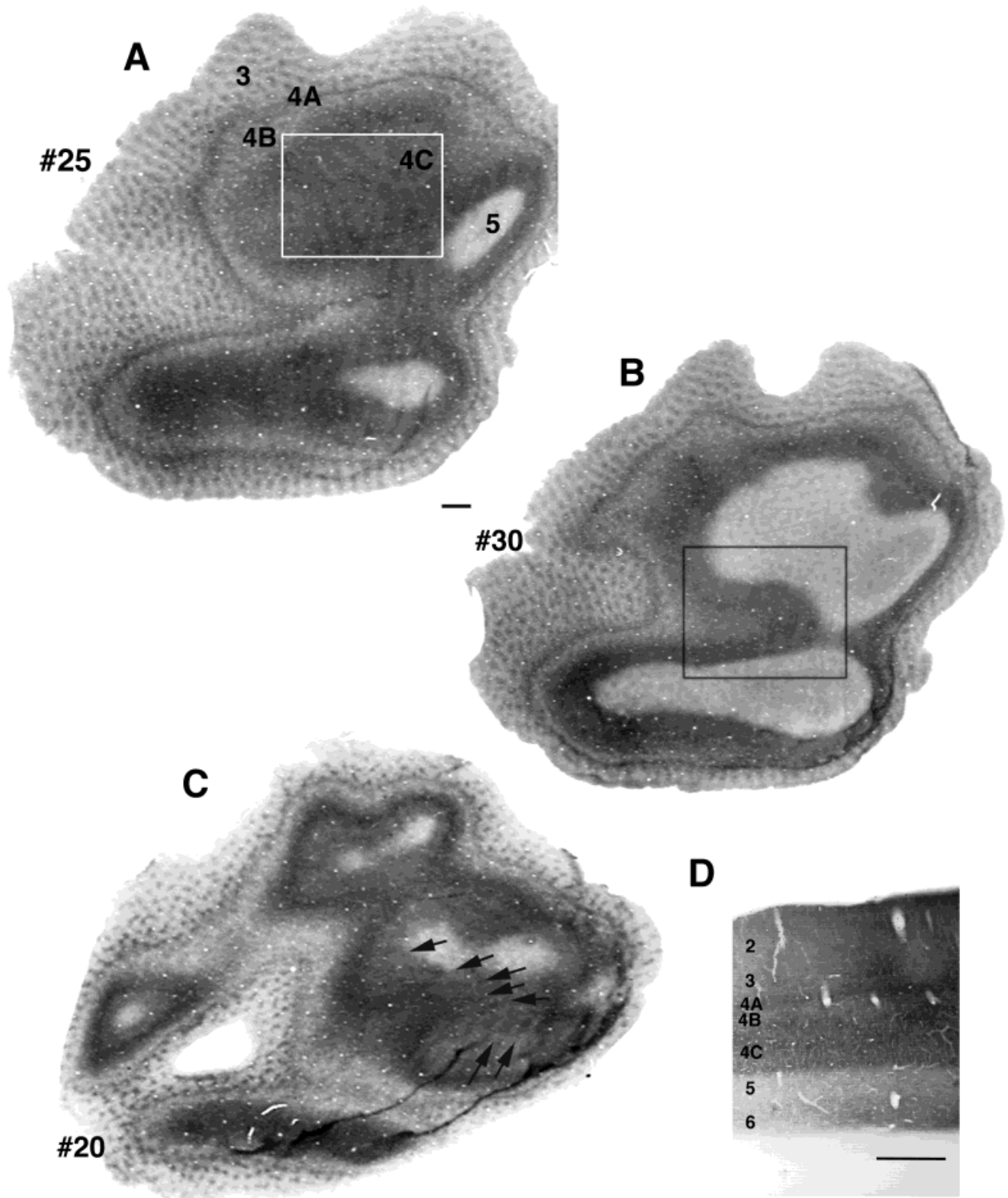


Fig. 2. CO staining in V1 of strabismic monkeys. **A,B:** Tangential sections from the occipital operculum from monkey PW. In these as all other sections from animals PW and SY, anterior is to the left; numbers indicate position in sequence beginning at pial surface. Note alternating light and dark stripes in layer 4C. **C:** CO-stained section

from monkey SY, showing similar, but less distinct, patterns (arrows mark dark stripes) to those seen in PW. **D:** Coronal section from monkey PW. White box in A identifies region shown in Figure 3A–C; black box in B identifies region shown in Figure 3D and E. Scale bars = 1 mm for A–C, 0.5 mm for D.

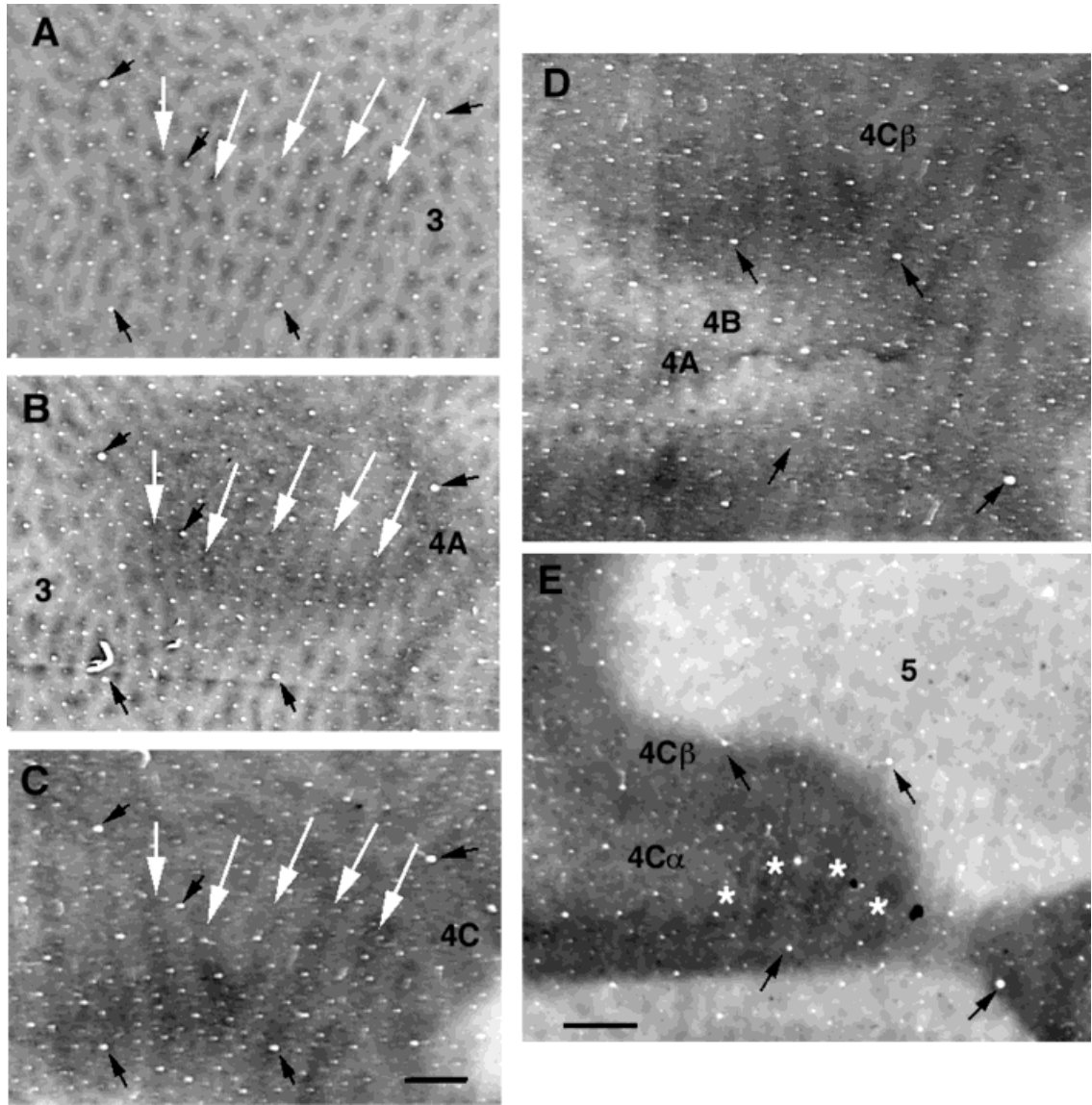


Fig. 3. Details of CO staining in layer 4 of strabismic monkey PW. Sections through layer 3 (A), 4A (B), and 4C (C) aligned to blood vessels marked by black arrows. White arrows mark dark stripes in layer 4Cb; these match every other row of blobs in layer 3 and stripes

in layer 4A. Solid stripes in most of layer 4C (D) and stripes in deepest part of layer 4C (E; marked by asterisks) consist of paired thin dark stripes with paler center. Scale bar = 1 mm.

keys however, faint stripes can be seen in all cortical layers but are most pronounced in layers 3 through 5. Figure 4A and B illustrates sections from monkey PW, and Figure 4C shows a section from SY. These stripes resemble thin OD columns in their general form, and they have a center to center spacing of about 0.4 mm ( $0.41 \text{ mm} \pm 0.01 \text{ SEM}$  for both animals); this suggests that both eyes' columns are represented. The dark stripes do not have sharp borders; the width of the stripes was measured by using NIH-Image to plot mean grayscale density as averaged over an 8-pixel-wide line drawn perpendicular to the stripes. The resulting plot was roughly sinusoidal, and the width of the dark stripes was measured at half-height. The widths of the dark components are  $0.24 \pm 0.01 \text{ mm}$  (SE) for both

animals. The most straightforward explanation for such a pattern would be cell loss in the pale stripes, but counts of all cells from dark and light stripes yield equivalent cell densities in dark and pale stripes, with  $61.88 \text{ cells}/100 \mu\text{m}^2 (\pm 2.74)$ , and  $67.38 \text{ cells}/100 \mu\text{m}^2 (\pm 3.16)$ , respectively. These means are not significantly different. The difference between dark and light stripes appears to be due to the intensity of staining of individual cells, presumably reflecting different rates of protein synthesis, or possibly differing numbers of neurons relative to glia. The same pattern is seen in Nissl-stained sections from monkey SY (Fig. 4C). The stripes are too faint to be visible in coronal sections.

The relation of the Nissl stripes to the ocular dominance column organization as derived from the CO pattern is

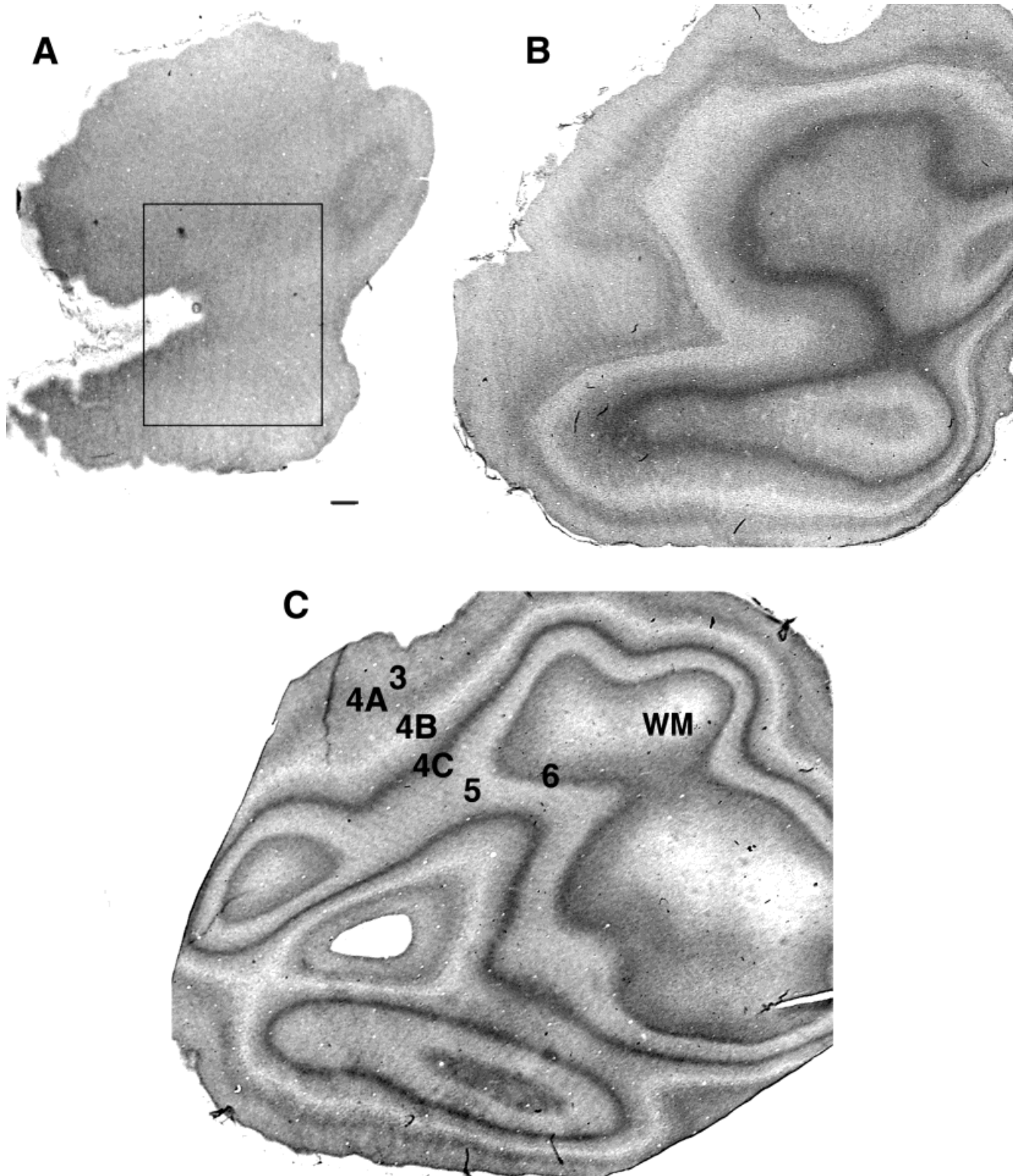


Fig. 4. Nissl staining in strabismic monkeys. **A:** Layer 3 of monkey PW. **B:** Layers 1-6 in monkey PW. **C:** Section through all layers to white matter in monkey SY. Box in A marks the region shown at higher magnification in Figure 5. Scale bar = 1 mm.

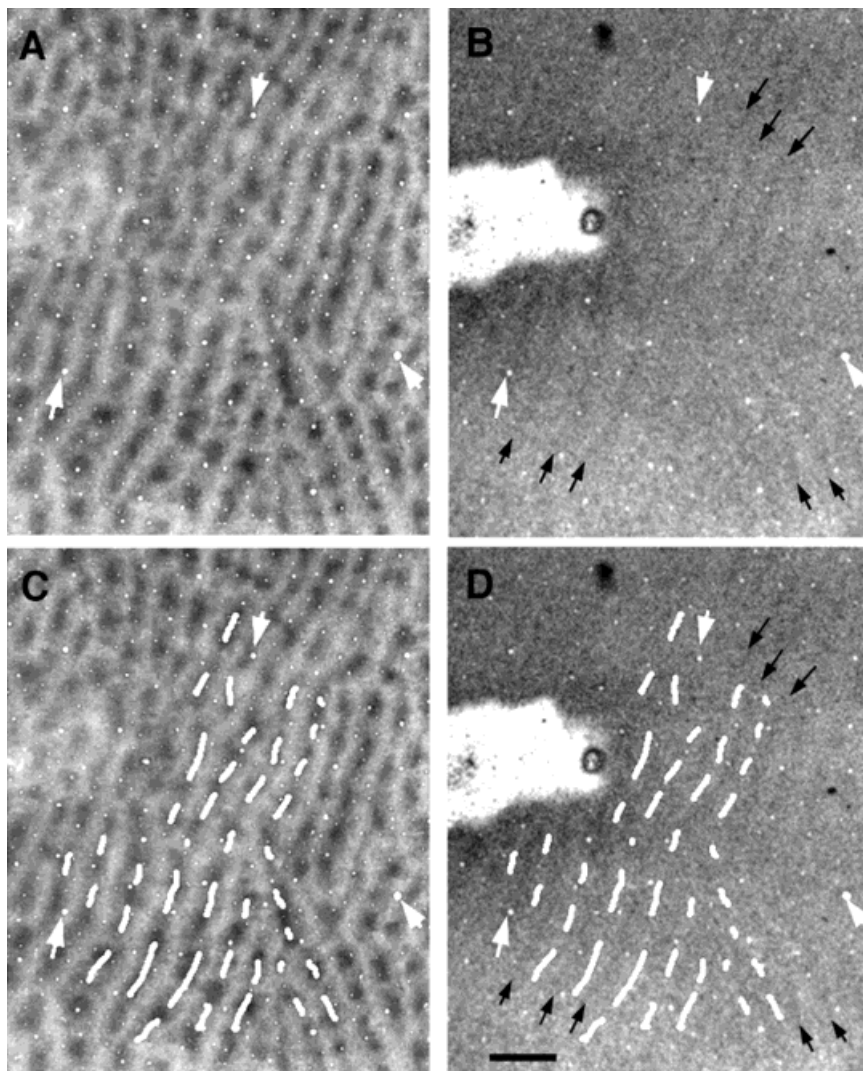


Fig. 5. Relation of stripe patterns in Nissl staining to OD columns. **A:** CO staining in layer 3 of monkey PW. **B:** Semi-adjacent section stained for Nissl substance; black arrows mark dark Nissl stripes. **C:** Same section as in A, with white lines drawn over dark CO regions marking

OD column centers. **D:** Section in B with lines from C marking OD column centers superimposed. Dark stripes marked by black arrows interdigitate with white lines. White arrowheads mark blood vessels used for section alignment. Scale bar = 1 mm.

illustrated in Figure 5. Semi-adjacent CO (Fig. 5A) and Nissl sections (Fig. 5B; black arrows mark dark Nissl stripes) from monkey PW are illustrated. Broken white lines connecting the blob centers (the centers of ocular dominance columns) were drawn on the CO section (Fig. 5C) and were then superimposed on the Nissl section (Fig. 5D); white arrows mark blood vessels used for section alignment); the lines interdigitate with the dark Nissl-stained stripes.

Although CO histochemistry indicates that overall metabolic activity is greater at the centers of OD columns, Nissl staining is darker at the borders of OD columns.

### Calbindin

The 28-kDa vitamin D-dependent calcium binding protein calbindin-D is expressed primarily by interneurons, and the normal immunoreactivity of the neuropil to calbindin antibody forms an irregular matrix in layer

3 (Fig. 1) that avoids the CO blobs (van Brederode et al., 1990; Carder et al., 1996). In experimentally strabismic monkeys, calbindin immunoreactivity in layer 3 and deeper forms stripes (Fig. 6). The stripes appear to be formed primarily by decreased calbindin expression in the neuropil between CO blobs at the centers of OD columns. In monkey PW (Fig. 6A,B,D), the dark calbindin-immunoreactive stripes are clear and narrow in layers 3 and 4B. The region shown in Figure 6C was taken from the region indicated by the box in Figure 6B, but from a more superficial section to show a greater extent of layer 3. In monkey SY (Fig. 6D), the dark stripes (marked by arrow) are less clear and appear wider in many areas than those in PW, but no section reacted to demonstrate calbindin provides a wide enough view of layer 3 to visualize the calbindin pattern optimally. Calbindin labeling in layer 4B in monkey SY appears to form broad, indistinct stripes. Although in-

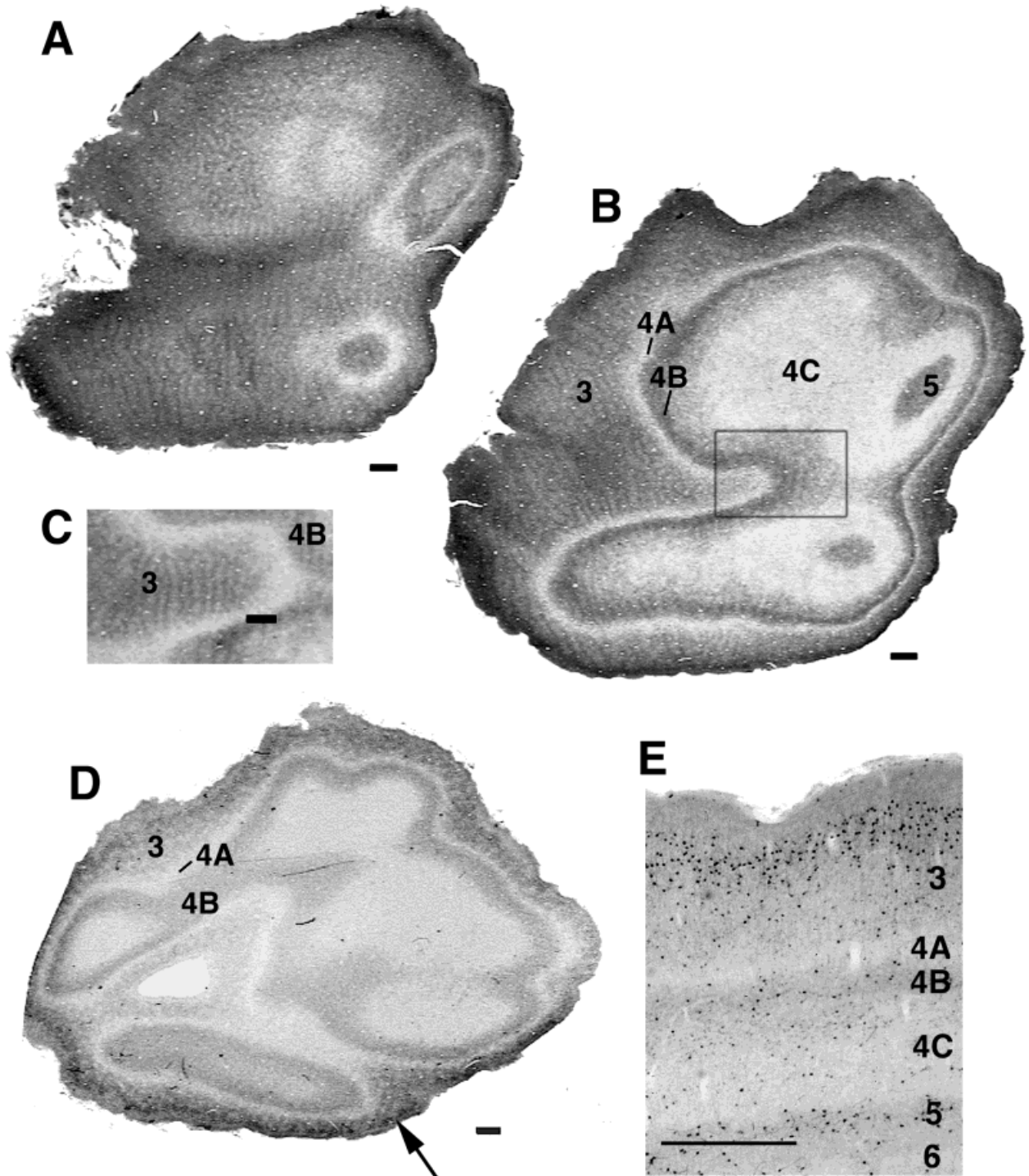


Fig. 6. Calbindin expression. **A:** Section showing calbindin immunoreactivity in layers 3 to 4B. **B:** Section extending to layer 5 from monkey PW. Box indicates region from a slightly more superficial section enlarged in **C** to show detail of calbindin immunolabeling in

layer 3 of monkey PW. **D:** Section extending to layer 4C from monkey SY. Arrow indicates relatively distinct stripes in layer 3. **E:** Coronal section from PW. Scale bars = 1 mm for A–D, 0.5 mm for D.

homogeneities are visible in calbindin immunolabeling of the superficial layers, no clear stripes can be seen in coronal section from monkey PW (Fig. 6E).

The dark and pale stripes of calbindin immunoreactivity are compared with the OD column structure in Figure 7. As in Figure 5, OD structure is revealed with CO staining in a

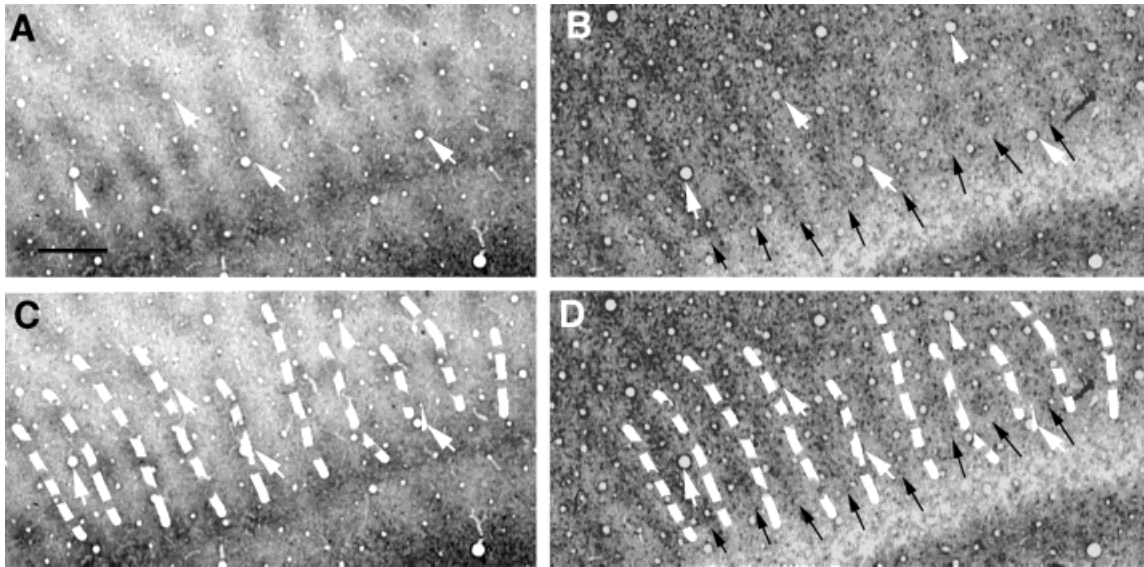


Fig. 7. Relation of stripe patterns in calbindin immunoreactivity to OD columns. **A:** CO staining in layer 3 of monkey PW. **B:** Adjacent section reacted with antibody against calbindin. Black arrows mark dark stripes of calbindin immunoreactivity. **C,D:** OD column centers

are marked by the dashed white line on the CO section, and OD centers are superimposed on calbindin section. White arrows mark blood vessels used for alignment. Scale bar = 1 mm.

nearby section (Fig. 7A,C). High calbindin expression (as indicated by thin black arrows in Fig. 7B,D) interdigitates with the OD column centers (indicated by broken white lines). Thus higher calbindin expression occurs at the OD column borders, as was the case for Nissl staining.

### Neurofilament immunoreactivity: SMI 32

Immunoreactivity for the pyramidal cell neurofilament protein epitope labeled by the SMI32 antibody in normal animals (Fig. 1) is particularly pronounced in small clusters of dendrites in the superficial layers. The clusters (green patches in Fig. 1, bottom panel of middle column), are not correlated with the CO pattern; this can be seen in the lower right-hand panel of Figure 1. Staining is also dense in neurons in layers 4B, 5, and 6, although faint immunoreactivity of dendrites can be seen in other layers, including 4C, where pyramidal cell bodies are scarce. Figure 8 shows tangential sections from the strabismic monkeys. In both animals, the normal patchy pattern has been replaced by rather striking stripes composed of immunoreactive patches that are separated by thin unstained strips (also see Fig. 9B). Rows of dense labeling alternate with paler rows, especially along the representation of the horizontal meridian, but even the less heavily immunostained stripes contain appreciable labeling in their centers. Sections taken from deeper layers (Fig. 8C) show the stripes extending into layer 4C, but fading out in layer 5. Viewed in coronal section (Fig. 8D), the immunoreactivity for SMI 32 appears patchy in layer 3, but the distinct unstained border strips that separate the thicker immunoreactive stripes are not apparent.

The OD structure is superimposed on SMI32 immunoreactivity in Figure 9. As in Figures 5 and 7, CO staining is used to mark OD column centers (Fig. 9A,C) and is compared with nearby SMI32-immunoreacted sections (Fig. 9B,D). The SMI32-positive stripes coincide with the OD column centers (marked by broken white lines),

whereas the narrow unstained strips (marked by black arrows in B and D) fall precisely at the OD column borders.

Figure 10 compares the alternate dark and pale OD columns seen with CO in layer 4C $\beta$  (Fig. 10A) with the SMI32 pattern of alternate stripes of greater and lesser density in layer 3 (Fig. 10B). The white arrows mark the less heavily immunolabeled SMI32 stripes, and the arrows are superimposed on the CO section in Figure 10A. The less densely labeled SMI32 stripes correspond to the dark CO columns. Thus, the OD columns of one eye are more intensely immunoreactive for SMI32 but show less CO activity in layer 4C $\beta$ . Black arrows mark blood vessels used for section alignment.

### Myelin staining

We observed subtle stripe patterns in wet, unstained sections through layer 4 from our strabismic monkeys. Horton and Hocking (1997) reported similar patterns in sections of V1 from monocularly enucleated monkeys, and these patterns represented the distribution of myelinated fibers. LeVay et al. (1975) originally reported an OD-related pattern of thick myelinated and thin pale stripes using the Liesegang silver stain in sections of layer 4C of visually normal monkeys. Subsequently, this pattern was found to be altered by visual deprivation (LeVay et al., 1980), resulting in layer 4C showing alternating thick and thin dark stripes separated by very thin pale stripes. The thick dark stripes were those of the untreated eye, and the thin dark stripes were those of the treated eye. They also found thick dark and thin pale stripes induced in layer 5, where the pale stripes aligned with the thin dark stripes of layer 4. Although Horton and Hocking (1997) found somewhat different patterns of staining using the Liesegang and Gallyas stains, we chose to use the Gallyas stain, as our sections had by then been stored for an extended period and this stain had previously proved to be fairly

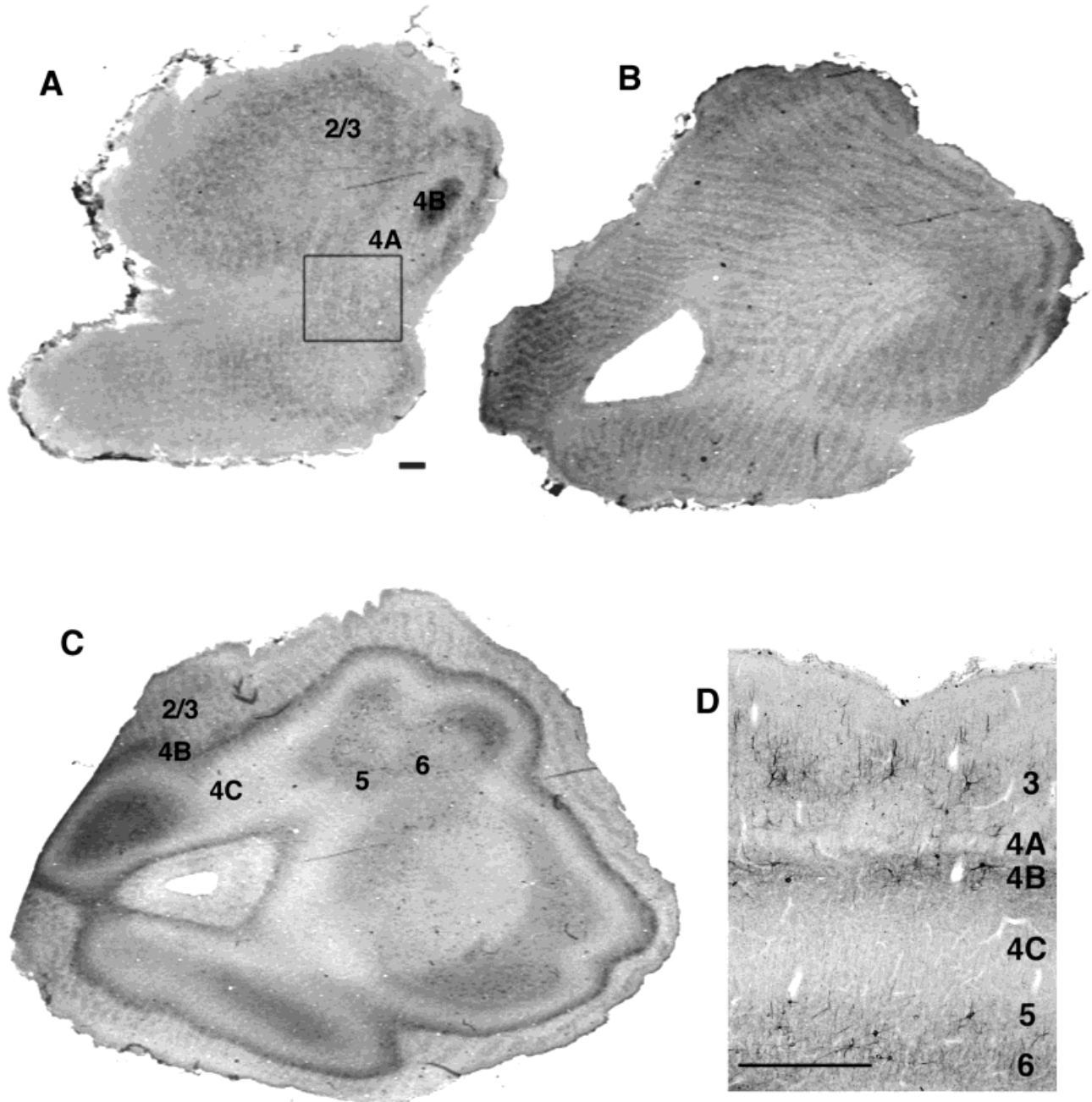


Fig. 8. Neurofilament expression as labeled by immunoreactivity to SMI32. **A:** Section from monkey PW. **B, C:** Sections from monkey SY. Stripe pattern extends through layer 4C. **D:** Coronal section from monkey PW. Box in A indicates region shown at higher magnification in Figure 9. Scale bars = 1 mm for tangential sections A–C, 0.5 mm for D.

reliable under such conditions. Figure 11 illustrates the Gallyas staining pattern seen in monkey PW. The normal pattern of broad dark stripes separated by thinner pale stripes is visible in layer 4C (indicated by the arrows in Fig. 11), but slightly thinner stripes continue superficially through layer 3 and are also visible in layer 5. The stripes have a periodicity suggesting that each eye's columns are represented by dark stripes. The staining in layer 6 is

quite uneven, but we find no consistent stripe pattern in this material. We believe this poor staining in layer 6 most likely occurred because the sections were stored in phosphate buffer for a long period prior to Gallyas staining.

We compared the Gallyas stripes from layers 3 and 4B with those observed in a nearby, but more superficial, Nissl-stained section. The Nissl section was chosen for comparison in this instance rather than the CO as the OD

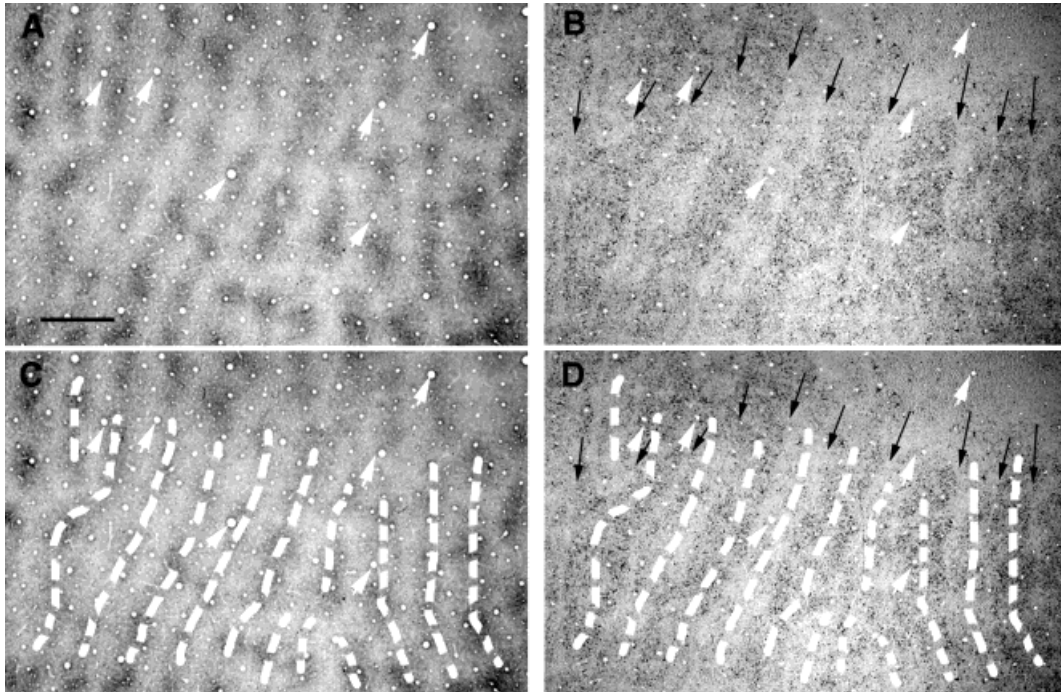


Fig. 9. Relation of stripe patterns in SMI32 neurofilament immunoreactivity to OD columns. **A:** CO staining in layer 3 of monkey PW. **B:** Adjacent section reacted with SMI32. Black arrows mark unstained stripes. **C,D:** OD column centers are marked on CO section, and OD centers are superimposed on SMI32 section. White arrows mark blood vessels used for alignment. Scale bar = 1 mm.

columnar structure is not readily apparent in either the more superficial CO section blobs or in the next deeper CO section through layer 4. In Figure 12A, black arrows mark the thin dark Gallyas stripes. A slightly more superficial Nissl-stained section is shown in Figure 12B, with the dark Nissl stripes marked by thin white arrows. In Figure 12C and D, the two sets of arrows have been placed in register, using the same blood vessels as fiducial marks (large white arrowheads) and superimposed on the Gallyas-and Nissl-stained sections, respectively. The black and white arrows interdigitate. Because the dark Nissl stripes coincide with the OD column borders, this suggests that the dark myelin-stained stripes lie at the OD column centers.

## DISCUSSION

In strabismic monkeys, each eye views a different part of the visual world, rather than converging on the same region. Where a binocularly activated neuron should normally receive highly correlated activation from the two eyes, it presumably receives uncorrelated input in strabismus (Löwel, 1994). This means that the balance of competitive, and perhaps cooperative, interactions between the afferents from the two eyes may be altered, although each eye should drive a cortical column of normal width. Electrophysiological investigations of neuronal properties in V1 of strabismic monkeys do find alterations in ocular dominance, such that few neurons show strong binocular activation, whereas the deviating and non-deviating eyes drive approximately equal numbers of neurons (Crawford and von Noorden, 1979; Wiesel, 1982; Kiorpes et al., 1998).

Only when pronounced amblyopia is present is there a shift in eye dominance away from the deviating eye (Kiorpes et al., 1998).

Neurons at the centers of ocular dominance columns should always display strong monocular bias by virtue of both the columnar input from the geniculorecipient layers and the direct input to the blobs from the intercalated layer neurons of the LGN itself. The binocular non-blob neurons receive more mixed eye input (Lachica et al., 1992; Yoshioka et al., 1994) and may become increasingly susceptible to modification with increasing distance from the ocular dominance column center. Our examination of markers for specific classes of neurons in V1 of strabismic monkeys revealed a number of alterations, particularly in the superficial layers, that may be related to the lack of binocular responsiveness found in cortical neurons in these animals. Most of these effects are seen at OD column borders.

In experimentally strabismic animals, labeling for CO and classes of interneurons that are normally associated with OD column centers reveals variable ocular dominance-related patterns in the geniculate input layers of V1, but there is no suggestion of OD columns of unequal width. Striking reorganization is seen in the expression of several other molecules outside the geniculorecipient layers of V1, as might be expected of a manipulation that alters binocular interactions; these altered patterns are represented schematically in Figure 13. Specifically, the expression of the SMI32-immunolabeled nonphosphorylated epitope on neurofilament proteins is high within pyramidal cells located along the center of the long axis of an ocular dominance column, but these dark stripes are

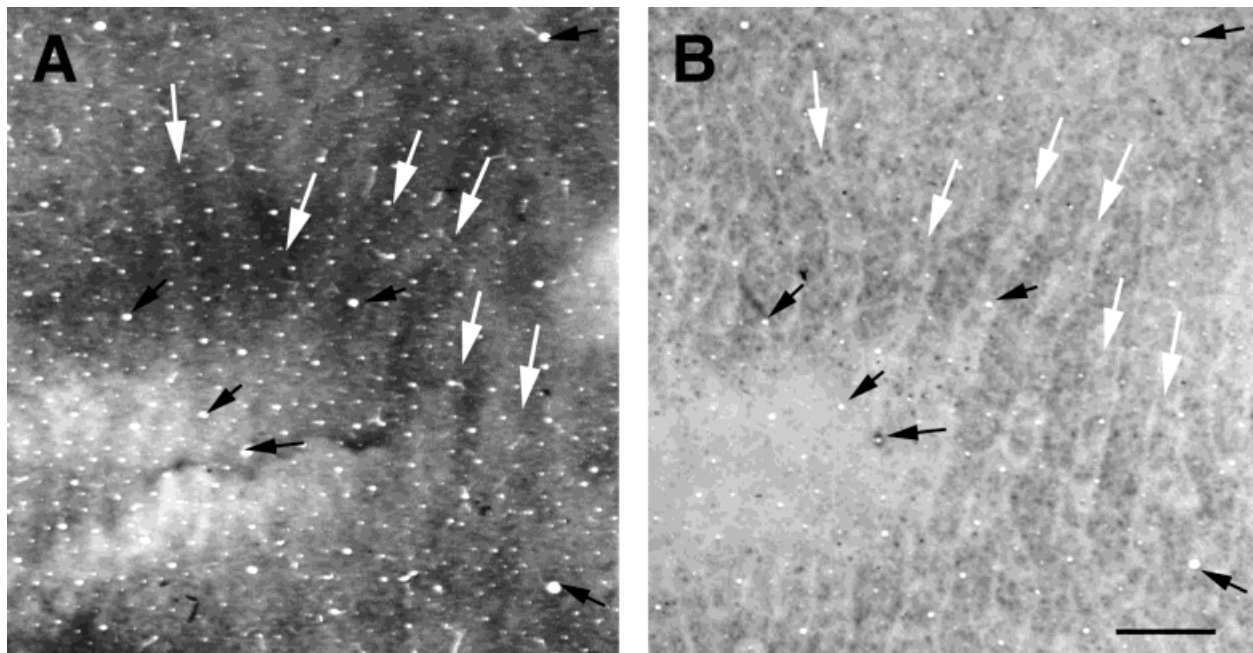


Fig. 10. Relation of the dark CO stripes in layer 4C of monkey PW (A) to the more darkly reacted SMI32-positive stripes in layer 3 (B). The centers of the paler SMI stripes have been marked with white arrows and superimposed on the CO section. Black arrows mark the blood vessels used for section alignment. Scale bar = 1 mm.

flanked by distinct unstained strips at OD column borders. These stripes extend through layers 3–5. In general, there is relatively decreased expression of the calcium binding protein calbindin within the processes of interneurons lying along the center of an ocular dominance column, but higher levels of expression of calbindin at the borders of ocular dominance columns. Nissl staining reveals stripes that exactly coincide with the calbindin stripes. Staining for myelin produces stripes in layers 3–5 that interdigitate with those seen in Nissl-stained and calbindin-immunoreacted material and therefore aligns with the SMI32 dark regions along the core zones of OD columns.

Some of the markers we have studied are found in particular morphological classes of neuron, whereas others reflect general levels of activity. We can therefore consider what their altered expression suggests about the organization of binocular vision in normal and strabismic monkeys. The existence of stripes in the Nissl-stained material is particularly interesting, as few alterations of visual function less severe than monocular enucleation (Haseltine et al., 1979) have been shown to produce such patterns. We have no explanation for the systematic variation on Nissl staining that is apparently not due to changes in the packing density of cells, but we suggest that the darker Nissl staining can be interpreted as indicating higher density of ribosomes that permit relatively higher rates of transcription of some protein or proteins at the OD column borders in strabismic monkeys. Similarly, the presence of stripes reflecting greater density of myelin at the OD column centers in all layers to, and possibly including, layer 6, seems to be consistent with greater activity of pyramidal cells located at monocular OD col-

umn centers relative to the normally binocular OD column borders in strabismic monkeys. Unfortunately, these patterns suggest little by way of explanation of how binocular vision is altered.

The mitochondrial enzyme CO is found in all neuronal classes and reflects overall activity levels. The CO staining pattern in the normally dark geniculate afferent recipient layer 4 is altered in strabismus, and the magnocellular and parvocellular recipient layers show different patterns. Thin, dark stripes aligned with the superficial layer blobs are seen in layer 4A. Layer 4C $\alpha$  is generally uniform, with hints of thin dark stripes at column centers, whereas alternate eye columns of normal width are dark in upper 4C $\beta$ . These dark stripes split into paired thin dark stripes in the same eye's columns in deepest 4C $\beta$ . The pattern of thin dark stripes representing each eye in layer 4C resembles the CO pattern described in newborn monkeys prior to visual experience (Horton and Hocking, 1996a). As OD columns in layer 4C of visually inexperienced monkeys have been demonstrated convincingly by Horton and Hocking, there is no requirement for normal visual experience to drive ocular dominance segregation; however, the sharpness of the column borders does increase with visual experience (Blasdel et al., 1995; Horton and Hocking, 1996a). It is possible that during the perinatal period the stellate cells at the monocular OD column core zones in layer 4C are most strongly driven and therefore metabolically active, whereas the border zones receive some overlapping input from both eyes. This binocular input may suppress, either directly or indirectly via interneurons, the spiny stellate cells of layer 4C and result in the less robust CO staining seen. Continuing correlated binocular competition would prune away the "wrong" eye's

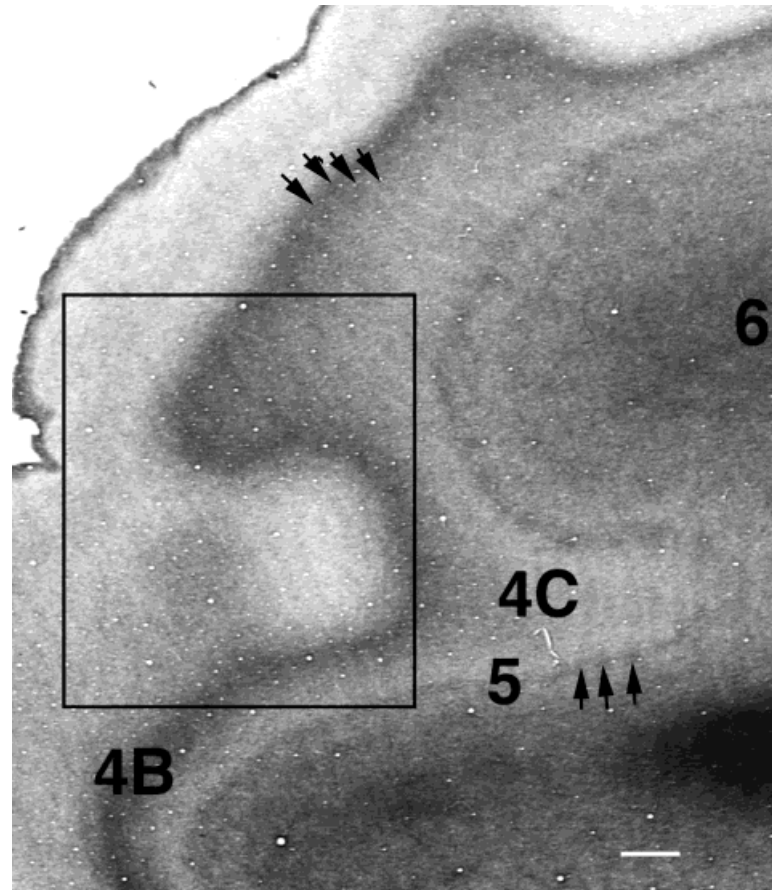


Fig. 11. Myelin staining in monkey PW. Dark stripes are visible in layers 3-5; black arrows indicate broader dark stripes in layer 4C. Box indicates region examined in Figure 12. Scale bar = 1 mm.

terminals to sharpen the OD column borders measured physiologically and result in more consistent monocular activation of neurons across the layer. Uniform CO staining would be produced from this stable activity. Uncorrelated binocular activity, as in strabismus, might not permit the pruning of terminals and might leave layer 4C in an immature state.

The pale staining of one eye's columns in layer 4C $\beta$  is more challenging to explain. In our animals, the afferents terminating in the pale columns were functional, as we found that both left and right eyes were able to drive MT neurons physiologically (Kiorpes et al., 1996). Furthermore, the superficial layer continuation of these columns showed normal CO activity. Attempts to associate the dark CO stripes induced by abnormal visual experience with the eye providing input have met with conflicting results. Tychsen and Burkhalter (1997) have determined that the "spontaneous" OD columns seen in CO staining of strabismic monkeys are related to the eye of origin without regard for the quality of visual experience; they found that the dark CO stripes in both hemispheres are those receiving the crossed, nasal retinal projection. They suggest that the numerical superiority of the crossed projection as well as the slightly delayed development of the uncrossed projection put the uncrossed eye projection at a competitive disadvantage. Rearing without normal binoc-

ular vision could prevent or alter the maturation of synapses that would normally result in uniform CO activity. The results of Tychsen and Burkhalter suggest that the dark CO stripes in our material were the columns driven by the right, non-deviating eye. We cannot evaluate this suggestion because only the left hemispheres of our monkeys were examined in tangential sections.

A different pattern consisting of thin dark CO bands in layer 4 has recently been reported in monkeys made strabismic as adults by Horton and Hocking (1998). Horton and Hocking have identified the dark stripes as corresponding to the non-deviating eye. A similar pattern in layer 4C has been described by Hendrickson and colleagues (Hendrickson et al., 1987) as an inconsistent result of rearing with experimental anisometropia. This group identified the stripes as those of the anisometropic eye. Although there may be different mechanisms involved in causing the alterations in CO activity associated with various forms of abnormal vision, the question of which eye drives the dark stripes remains unsettled.

The CO-enriched blobs of the superficial layers receive afferents from the monocular intercalated layer neurons of the LGN, as well as vertically ascending projections from layer 4. As the blobs lie at the centers of the OD columns (Horton, 1984), they represent the location of the most monocularly biased neurons. The CO bridges also

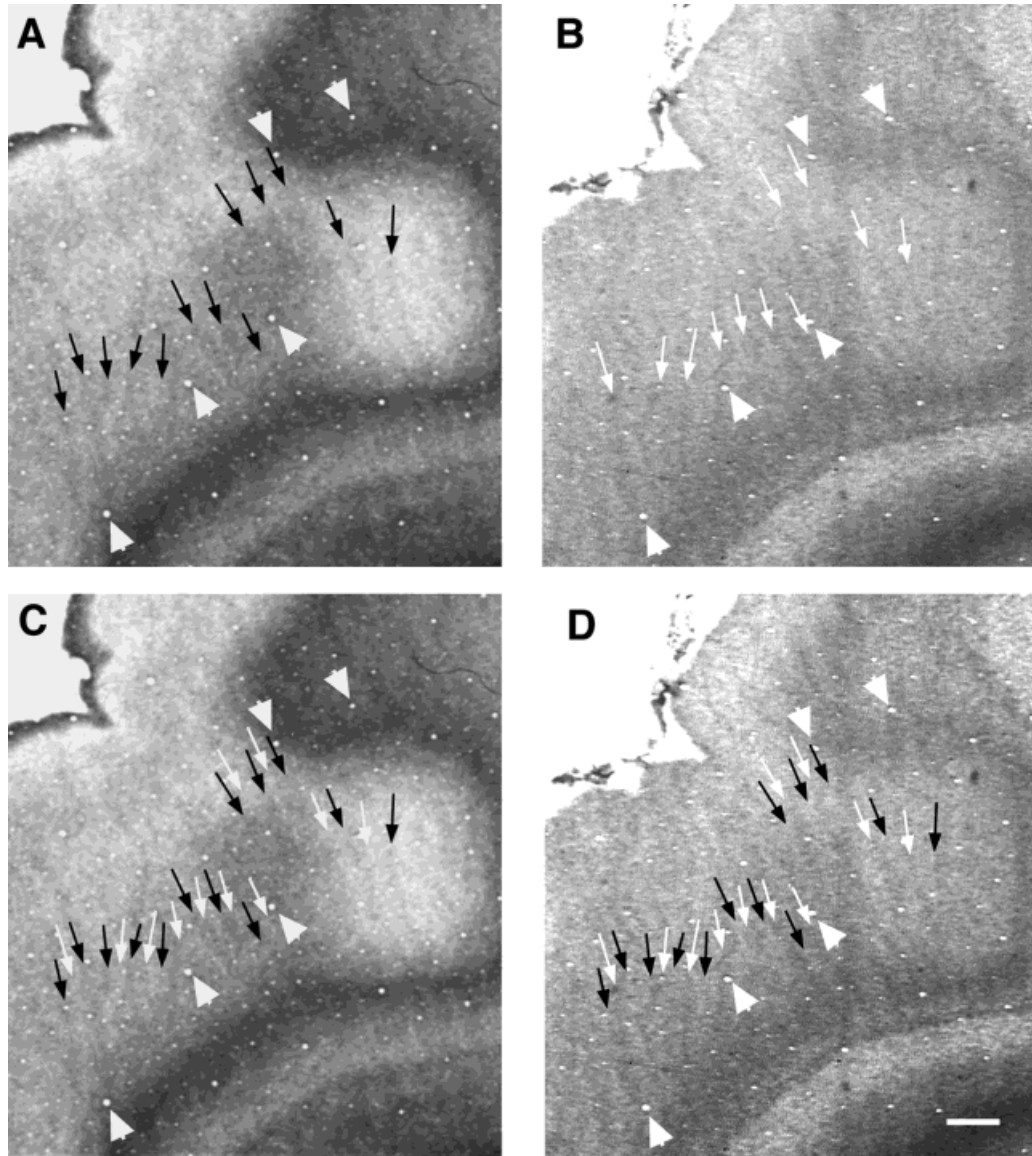


Fig. 12. Comparison of Nissl and myelin stripes in layer 3. **A:** Gallyas stain for myelin; large white arrowheads mark blood vessels used for section alignment; small white arrows mark dark stripes. **B:** Section taken from slightly more superficial level stained for Nissl sub-

stance. Small black arrows indicate dark stripes in layer 3. **C:** Gallyas-stained section and **(D)** Nissl-stained section, each with arrows marking Gallyas and Nissl stripes superimposed. Scale bar = 1 mm.

follow the centers of OD columns, and neurons located within these bridges are normally monocularly biased, but receive significant binocular input. Neurons farther from the ocular dominance column center, in the CO pale regions, presumably get more nearly equal driving and are binocularly responsive neurons.

In strabismic monkeys, these binocular neurons apparently become more strongly biased toward driving by one eye, as few strongly binocular neurons are found electrophysiologically. The shift toward monocular responses might be attributable to increased activation of inhibitory interneurons. For example, NADPH diaphorase histochemistry in strabismic monkeys produces patterns of neuropil staining that are indistinguishable from CO. As the larger NADPH diaphorase-containing neurons are

GABAergic interneurons that are preferentially associated with OD column centers (Sandell, 1986), they may play a role in suppressing non-preferred eye inputs onto monocularly biased, binocular neurons in strabismic monkeys. This suppression would drive the neuron's responsiveness toward the dominant eye.

Many of the inhibitory interneurons of the superficial layers in V1 contain one of the calcium binding proteins. The role of calcium binding proteins in neurons is not well understood, but they are known to be involved in buffering intracellular calcium levels (Baimbridge et al., 1982). This property might suggest that expression of calcium binding proteins, such as calbindin, would be related to high firing rates. As calbindin-containing neurons in V1 of macaques are typically GABAergic, the increased expression of cal-

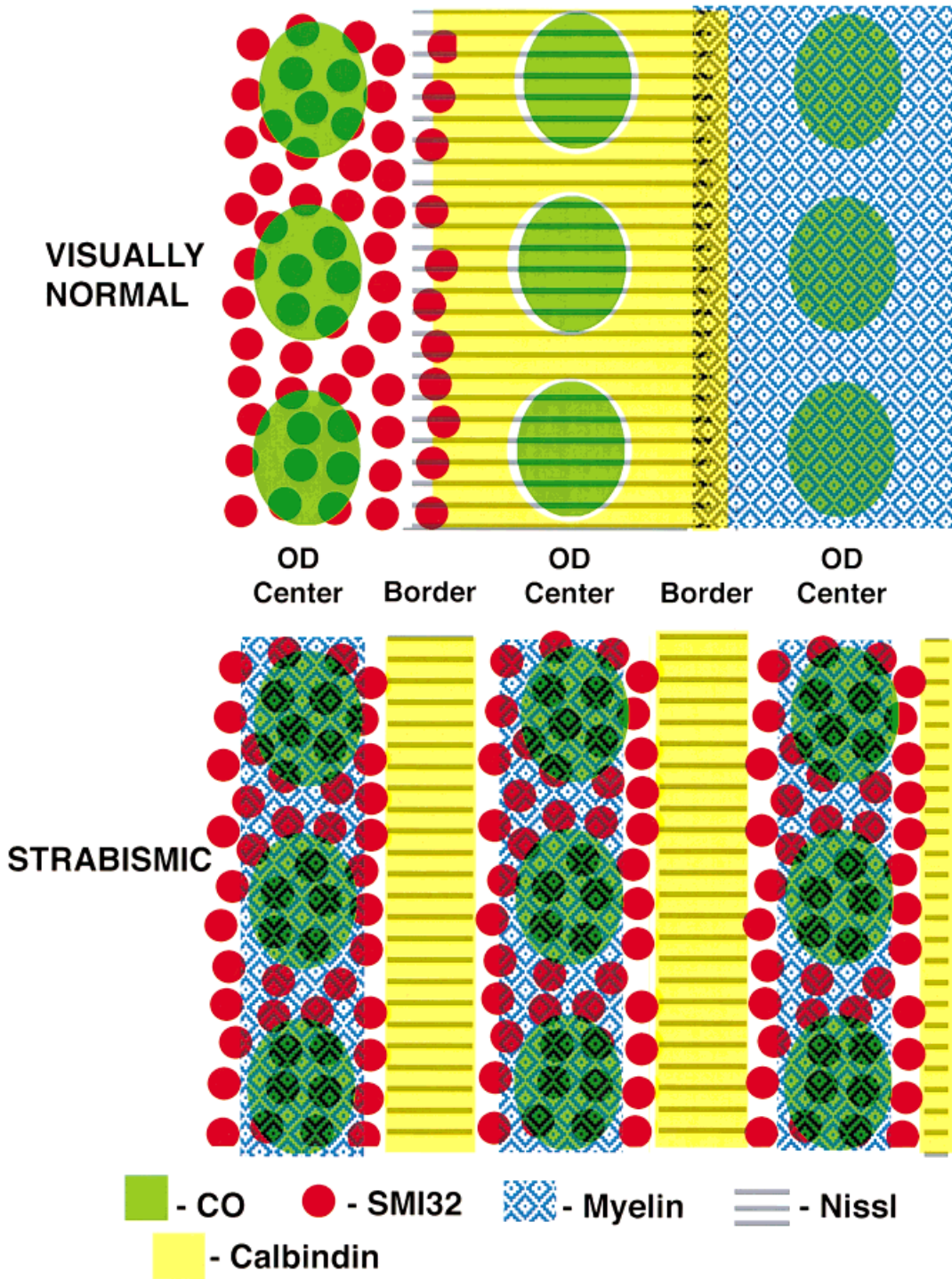


Fig. 13. Summary of labeling patterns obtained in the superficial layers of V1 in strabismic monkeys. The relation of each marker to CO is shown; CO blobs are indicators of the centers of ocular dominance columns.

bindin at OD column borders might indicate increased activity of these inhibitory interneurons. Calbindin is overexpressed in monkey V1 during the late prenatal and early postnatal periods, reaching adult levels by about 5 months after birth (Hendrickson et al., 1991). This early

postnatal immunolabeling of calbindin is particularly robust in the neuropil of interblob regions (Fenstermaker, unpublished observations), so its expression is sufficiently labile during early visual experience to be shaped by binocular interactions. Prior evidence of possible sensitivity

to binocular interactions in calbindin-containing neurons can be found in the fact that calbindin expression is decreased by monocular form deprivation in V1 but not the LGN (Mize et al., 1992).

Pyramidal cells are the main extragranular layer excitatory neurons of cortex, and those pyramidal cells that express the nonphosphorylated neurofilament protein epitope labeled by SMI32 are affected by strabismus. The somata and dendrites of these neurons typically form clusters in the superficial layers, and these clusters are distributed in no consistent relation to the CO blobs. We might expect that the cells located within blobs would be normally monocularly biased, whereas those outside blobs would be binocular. In strabismus, the expression of SMI32 disappears completely from pyramidal cells at the OD border zones, leaving distinct unstained strips between rows of patches of immunoreactive neurons. We can assume that the remaining immunoreactive neurons are strongly monocularly responsive, as few binocularly activated neurons are encountered electrophysiologically in strabismic animals. In both animals, although each eye's OD columns contain patches of neurons that are immunoreactive for SMI32, alternate rows contain less robust labeling, particularly within the representation of the horizontal meridian. This observation could be explained by the fact that strabismic individuals may consistently fixate with one eye, or alternate the eye used for fixation. When only one eye is used, amblyopia typically results (Kiorpes et al., 1989). Both of our monkeys alternated fixation but may have used one eye more consistently. It is interesting to note that the columns expressing less SMI32 were the columns that were darker in CO staining in layer 4C.

Pyramidal cells can be classified as projecting or local according to their axonal targets. The SMI32-immunoreactive pyramidal cells are known to project to other cortical areas (Hof et al., 1996). Sawatari and Callaway (2000) have reported that neurons of layer 4C $\beta$  make functional synaptic contact only with local pyramidal neurons in layer 3B but not with projection neurons. Thus, the decrease in SMI32 immunoreactivity in a significant proportion of the layer 3 cells probably results from synaptic interactions at earlier stages of processing in layer 3.

Our results suggest a mechanism by which strong binocular responses are lost as a result of strabismus. It is possible that in strabismic individuals, non-correlated excitation of calbindin-containing neurons located at OD column borders could produce overall higher levels of activity in these neurons. This situation could occur if each eye's input produced an action potential in the calbindin neurons, whereas in the normal case, correlated inputs would sum to a single action potential. Increased activity of the calbindin-containing interneurons should result in increased inhibition of nearby pyramidal cells. These pyramidal cells at OD column borders would rarely, if ever, receive sufficient excitation to fire and might reduce expression of the neurofilament proteins recognized by SMI32. Because the SMI32 antibody recognizes a non-phosphorylated epitope, the loss of immunoreactivity without loss of cells probably indicates a change in phosphorylation of the cells at the OD column borders.

The paler myelin staining seen at OD border regions also suggests that pyramidal cells there are less active, although they are probably still present, as counts of Nissl-stained cells show no loss at column borders. Al-

though monocularly responsive neurons in V1 could still provide convergent input onto neurons in higher order cortical areas to produce binocular responses, it appears that direct input from binocular neurons in V1 is required for normal binocular vision.

Finally, no electrophysiological studies of V1 in strabismic monkeys have reported any reduction overall in numbers of encountered units, or distinct zones of unresponsiveness that might correspond to the SMI32-depleted OD border strips. Our results suggest that robust single-unit responses will prove to be absent from the transition zones between left and right eye columns, although faint binocular background activity may be present.

## ACKNOWLEDGMENTS

J.A.M. was the recipient of a Howard Hughes Medical Institute Investigatorship.

## LITERATURE CITED

- Aoki C, Fenstemaker S, Go C-G, Lubin M. 1993. Nitric oxide synthase in the visual cortex of monocular monkeys as revealed by light and electron microscopic immunocytochemistry. *Brain Res* 620:97-113.
- Baimbridge KG, Miller JJ, Parkes CO. 1982. Calcium-binding protein distribution in the rat brain. *Brain Res* 239:519-525.
- Blasdel G, Obermayer K, Kiorpes L. 1995. Organization of ocular dominance and orientation columns in the striate cortex of neonatal macaque monkeys. *Vis Neurosci* 12:589-603.
- Campbell MJ, Morrison JH. 1989. Monoclonal antibody to neurofilament protein (SMI-32) labels a subpopulation of pyramidal neurons in the human and monkey neocortex. *J Comp Neurol* 282:191-205.
- Carder RK, Leclerc SS, Hendry SHC. 1996. Regulation of calcium-binding protein immunoreactivity in GABA neurons of macaque primary visual cortex. *Cereb Cortex* 6:271-287.
- Celio MR, Schärer L, Morrison JH, Norman AW, Bloom FE. 1986. Calbindin immunoreactivity alternates with cytochrome C oxidase-rich zones in some layers of the primate visual cortex. *Nature* 323:715-717.
- Crawford MLJ, von Noorden GK. 1979. The effects of short-term experimental strabismus on the visual system in *Macaca mulatta*. *Invest Ophthalmol Vis Sci* 18:496-505.
- Dawson TM, Bredt DS, Fotuhi M, Hwang P, Snyder SH. 1991. Nitric oxide synthase and neuronal NADPH diaphorase are identical in brain and peripheral tissues. *Proc Natl Acad Sci USA* 88:777-7801.
- Gallyas F. 1979. Silver staining of myelin by means of physical development. *Neurosci Res* 1:203-209.
- Haseltine EC, deBruyn EJ, Casagrande CA. 1979. Demonstration of ocular-dominance columns in Nissl-stained sections of monkey visual cortex following enucleation. *Brain Res* 176:153-158.
- Hendrickson AE, Movshon JA, Eggers HM, Gizzi MS, Boothe RG, Kiorpes L. 1987. Effects of early unilateral blur on the macaque's visual system. II. Anatomical observations. *J Neurosci* 7:1327-1339.
- Hendrickson AE, van Brederode JFM, Mulligan KA, Celio MR. 1991. Development of the calcium-binding proteins parvalbumin and calbindin in monkey striate cortex. *J Comp Neurol* 307:626-646.
- Hendry SCH, Bhandari MA. 1992. Neuronal organization and plasticity of adult monkey visual cortex: immunoreactivity for microtubule-associated protein. *Visual Neurosci* 9:445-459.
- Hendry SHC, Carder RK. 1993. Neurochemical compartmentation of monkey and human visual cortex: similarities and variations in calbindin immunoreactivity across species. *Vis Neurosci* 10:1109-1120.
- Hendry SHC, Jones EG, DeFelipe J, Schmechel D, Brandon C, Emson PC. 1984. Neuropeptide-containing neurons of the cerebral cortex are also GABAergic. *Proc Natl Acad Sci USA* 81:6526-6530.
- Hof PR, Ungerleider LG, Webster MJ, Gattass R, Adams M, Sailstad CA, Morrison JH. 1996. Neurofilament protein is differentially distributed in subpopulations of corticocortical projection neurons in the macaque monkey visual pathways. *J Comp Neurol* 376:112-127.
- Hope BT, Michael GJ, Knigge KM, Vincent SR. 1991. Neuronal NADPH diaphorase is a nitric oxide synthase. *Proc Natl Acad Sci USA* 88:2811-2814.

- Horton JC. 1984. Cytochrome oxidase patches: a new cytoarchitectonic feature of monkey visual cortex. *Philos Trans R Soc Lond Biol* 304:199–253.
- Horton JC, Hocking DR. 1996a. An adult-like pattern of ocular dominance columns in striate cortex of newborn monkeys prior to visual experience. *J Neurosci* 16:1791–1807.
- Horton JC, Hocking DR. 1996b. Intrinsic variability of ocular dominance column periodicity in normal macaque monkeys. *J Neurosci* 16:7228–7339.
- Horton JC, Hocking DR. 1997. Myelin patterns in V1 and V2 of normal and monocularly enucleated monkeys. *Cereb Cortex* 7:166–177.
- Horton JC, Hocking DR. 1998. Experimental strabismus reduces metabolic activity in ocular dominance columns serving the deviated eye. *Soc Neurosci Abstr* 24:260.
- Hubel DH, Wiesel TN. 1965. Binocular interaction in striate cortex of kittens reared with artificial squint. *J Neurophysiol* 28:1041–1059.
- Jones EG, Hendry SCH, DeFelipe J. 1987. GABA-peptide neurons of the primate cerebral cortex: a limited cell class. New York: Plenum Press.
- Kiorpes L, Movshon JA. 1996. Amblyopia: a developmental disorder of the central visual pathways. *Cold Spring Harbor Symp Quant Biol LXI*:39–48.
- Kiorpes L, Boothe RG. 1980. The time course for the development of strabismic amblyopia in infant monkeys (*Macaca nemestrina*). *Invest Ophthalmol Vis Sci* 19:841–845.
- Kiorpes L, Kiper DC, O'Keefe LP, Cavanaugh JR, Movshon JA. 1998. Neuronal correlates of amblyopia in the visual cortex of macaque monkeys with experimental strabismus and amblyopia. *J Neurosci* 18:6411–6424.
- Kiorpes L, Walton PJ, O'Keefe LP, Movshon JA, Lisberger SG. 1996. Effects of early-onset strabismus on pursuit eye movements and on neuronal responses in area MT of macaque monkeys. *J Neurosci* 16:6537–6553.
- Kiorpes L, Carlson MR, Alfi D, Boothe RG. 1989. Development of visual acuity in experimentally strabismic monkeys. *Clin Vision Sci* 4:95–106.
- Lachica EA, Beck PD, Casagrande VA. 1992. Parallel pathways in monkey striate cortex: Anatomically defined columns in layer III. *Proc Natl Acad Sci USA* 89:3566–3570.
- Leclerc SS, Carder RK. 1994. Neurochemical effects of monocular aphakia in supragranular layers of V1 of the adult macaque. *Soc Neurosci Abstr* 20:1577.
- LeVay S, Hubel DH, Wiesel TN. 1975. The pattern of ocular dominance columns in macaque striate cortex revealed by a reduced silver stain. *J Comp Neurol* 159:559–576.
- LeVay S, Wiesel TN, Hubel DH. 1980. The development of ocular dominance columns in normal and visually deprived monkey. *J Comp Neurol* 191:1–51.
- Löwel S. 1994. Ocular dominance column development: strabismus changes the spacing of adjacent columns in cat visual cortex. *J Neurosci* 14:7451–7468.
- Löwel S, Singer W. 1992. Selection of intrinsic horizontal connections in the visual cortex by correlated neuronal activity. *Science* 255:209–212.
- Mize RR, Luo Q, Tigges M. 1992. Monocular enucleation reduces immunoreactivity to the calcium-binding protein calbindin 28 kD in the Rhesus monkey lateral geniculate nucleus. *Vis Neurosci* 9:471–482.
- Murphy KM, Jones DG, Fenstermaker SB, Pegado VD, Kiorpes L, Movshon JA. 1998. Spacing of cytochrome-oxidase blobs in visual cortex of normal and strabismic monkeys. *Cereb Cortex* 8:237–244.
- Sandell JH. 1986. NADPH diaphorase histochemistry in the macaque striate cortex. *J Comp Neurol* 251:388–397.
- Sawatari A, Callaway EM. 2000. Diversity and cell type specificity of local excitatory connections to neurons in layer 3B of monkey primary visual cortex. *Neuron* 25:459–471.
- Tychsen L, Burkhalter A. 1992. Naturally-strabismic primate lacks intrinsic horizontal connections for binocular vision in striate cortex. *Soc Neurosci Abstr* 18:1455.
- Tychsen L, Burkhalter A. 1997. Nasotemporal asymmetries in V1: ocular dominance columns of infant, adult, and strabismic macaque monkeys. *J Comp Neurol* 388:32–46.
- Tychsen L, Lisberger SG. 1986. Maldevelopment of visual motion processing in humans who had strabismus with onset in infancy. *J Neurosci* 6:2495–2508.
- Tychsen L, Hanaway K, Burkhalter A. 1996. Axonal and dendritic circuits of V1 ocular dominance columns in normal and strabismic macaque. *Soc Neurosci Abstr* 22:1728.
- van Brederode JFM, Mulligan KA, Hendrickson AE. 1990. Calcium-binding proteins as markers for subpopulations of GABAergic neurons in monkey striate cortex. *J Comp Neurol* 298:1–22.
- von Noorden GK. 1980. Binocular vision and ocular motility. St. Louis, MO: Mosby.
- Wiesel TN. 1982. Postnatal development of the visual cortex and the influence of environment. *Nature* 299:583–591.
- Wong-Riley MTT. 1979. Changes in the visual system of monocularly sutured or enucleated cats demonstrable with cytochrome oxidase histochemistry. *Brain Res* 171:11–28.
- Yoshioka T, Levitt JB, Lund JS. 1993. Anatomical basis for channel interactions in macaque cortical visual area V1. *Invest Ophthalmol Vis Sci (Suppl)* 34:1173.
- Yoshioka T, Levitt JB, Lund JS. 1994. Independence and merger of thalamocortical channels within monkey primary visual cortex: anatomy of interlaminar projections. *Vis Neurosci* 11:467–489.
- Yoshioka T, Tigges M, Hendry SHC. 1996. Developmental plasticity of modules in macaque V1. *Soc Neurosci Abstr* 22:1728.